

# Analysis of the dynamics of the rolling process of multilayer viscoelastic bodies

Dariusz Rydz<sup>1\*</sup>, Mariusz Salwin<sup>2</sup>, Michał Pałęga<sup>1</sup>, Tomasz Chmielewski<sup>2</sup>

<sup>1</sup> Faculty of Production Engineering and Materials Technology, Czestochowa University of Technology, al. Armii Krajowej 19, 42-201 Czestochowa, Poland

<sup>2</sup> Faculty of Mechanical and Industrial Engineering, Warsaw University of Technology, ul. Narbutta 86, 02-524 Warszawa, Poland

\* Corresponding author's e-mail: mariusz.salwin@onet.pl

## ABSTRACT

The paper identifies deformations in layers of laminated composite sheets shaped in the rolling process. Rolling process of layered composites is a dynamic issue, for which the problem is to precisely determine the value of deformations of individual sheet components resulting from differences in their properties. The aim of this work was to determine the impact of delayed viscoelastic effects on increasing the computational accuracy of deformations of metal layers constituting the AlMg+Al1050+M1E layered composite. Three three-parameter Jeffreys models connected in parallel were used to analyze the course of changes in deformation of laminar composite layers. The presented test results refer to the determination of the deformation values in the rolling valley and the zone of delayed viscoelastic effects. The work showed that the solution used contributed to increasing the accuracy of the calculations.

**Keywords:** mathematical model, viscoelasticity, layered composites, rolling process.

## INTRODUCTION

Layered composite products are increasingly used in many industries. Expectations for the use of composite, layered materials often result in side effects, as well as technical, layered combinations of the materials' properties. It should be noted that the shared, detailed impact of the complex layering is small, which translates into costs resulting from the files. Composite layered materials are finding increasingly wider industrial and research applications [1–3]. The interest in this type of materials is most often due to economic reasons [4, 5]. This phenomenon can be used to develop metal-layered composite technology [6]. The process includes basic metal connection processes and their plastic-shaping consequences. There are many methods of joining metals [6], but in case of a problem, the combination of layers of small thickness is a problem. It is often necessary to supply metal materials in the plastic forming process. When shaping a layered

composite, problems arise with separating individual composite layers resulting from their different properties [7, 8].

Numerical modeling is based on the structural element method for characteristic parameters from one of the previous elements [9]. A definite alternative version that takes advantage of the use of plasticity [10, 11]. These solutions are not taken into account, but the delayed viscoelastic effects have final significance based on the amounts deformed in the form of laminated composite sheets [12]. Viscoelastic effects are noticeable immediately after the composite material releases the deformation zone [13, 14].

The dynamic rolling process is most often used to shape composite sheets. Therefore, the study analyzed the deformations of individual layers constituting the composite, both in the deformation zone and in the zone of delayed viscoelastic effects. Calculations based on the theory of viscoelasticity allow for the presentation of the full course of the deformation process of

the components of layered composites, including both the rolling valley and the mentioned zone of delayed viscoelastic effects, as shown in Figure 1.

The author of the paper proposed solutions for viscoelastic bodies, which were developed and discussed in [6]. This solution is a new approach to the analysis of the rolling process of layered composites. Taking into account delayed viscoelastic effects allows for precise determination of the values of deformations of materials constituting the composite. In most works, the differences between the set and permanent deformation were attributed only and exclusively to the stiffness of the rolling stand, which is not entirely correct. In this paper, the course of deformation changes in the rolling gap and in the zone of delayed viscoelastic effects was determined.

Even though viscoelastic solutions were discovered long ago, they are often used to analyze many phenomena. One example is the use of viscoelastic solutions described in [15] to analyze the behavior of a supported beam subjected to variable loads. The half-space reactions to the sleepers were replaced by an arrangement of identical springs placed under each sleeper. Another exciting solution based on viscoelasticity is using magneto-therm-viscoelastic surface waves in conductive layers, as presented in [16]. In this work, the dependence of strain rate and stress on time in media under initial load was considered. In subsequent works, viscoelastic solutions were used to identify material properties [17, 18]. Viscoelastic solutions are critical [19] and often used in works dealing

with biomechanics [20, 21], e.g., using elastography to measure the viscoelasticity of biological tissues or analyzing biodynamic skin tension lines for surgical cutting [22, 23]. In subsequent works directly related to the topic discussed in this work, the following were analyzed: the detachment of viscoelastic tapes adhering to a rigid flat substrate [24] and the reaction of the viscoelastic substrate to external impacts [25]. Despite such a wide range of viscoelastic application applications, more work is needed related to their use in the rolling process. This is mainly due to the specialized use of specific solutions and complicated mathematical descriptions. The effects of the discussed solutions resulted in this issue being taken up in work [6], where the rolling process of two-layer bimetal sheets was analyzed. The paper presents and discusses the dynamics of deformations occurring during cold rolling of flat two-layer products using solutions for viscoelastic bodies [6]. The presented work continues the considerations discussed in [6] related to using viscoelastic solutions to analyze the rolling process of layered composites composed of three layers [26, 27]. The use of viscoelastic solutions allows for analyzing the course of deformations of individual layers during the passage through the zone of intense deformations and their behavior in the zone of delayed viscoelastic effects, Figure 1 [28, 29]. The problem of dimensional accuracy of products made of layered composite materials is one of the main issues addressed in many research works [6, 30].

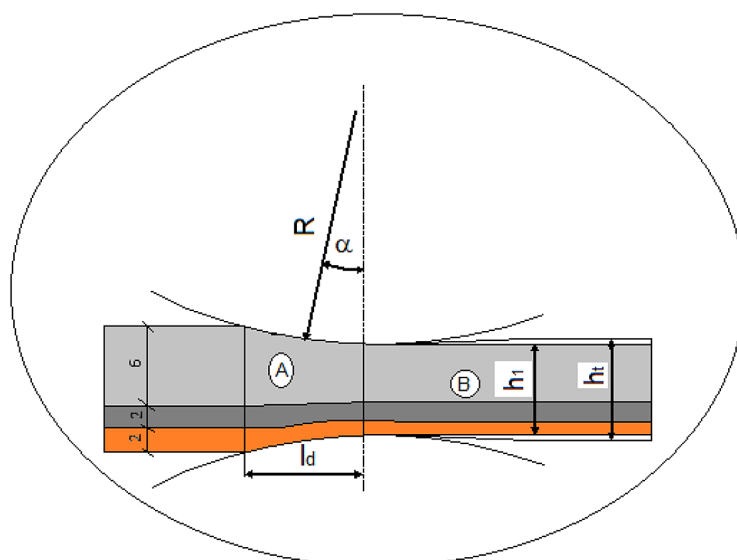


**Figure 1.** Scheme of the rolling process of viscoelastic layered composites divided into zones A - rolling trough (intense deformations), B – delayed viscoelastic effects;  $l_d$  – length of the rolling valley,  $h_1$  – total deformation in the rolling trough,  $h_2$  – total deformation in the zone of delayed viscoelastic effects

## MATERIAL AND METHODS

Three-layer composites obtained by explosive welding were used for the tests. The chemical composition of the materials used for joining is given in Table 1. The three-layer composites were joined by explosive welding. Figure 2 shows a view of a sample cut from the middle part of a joined composite sandwich sheet.

The first stage of the research was to check the durability and continuity of the connection areas of the sandwich composite components. Then, test samples with dimensions of 10×120×200 mm were cut from the joined sheet. The plastic shaping process was carried out on a duo rolling mill with a roll diameter of φ150 mm. The view of the rolling mill is shown in Figure 3. As part of the conducted research, it was planned to carry out the rolling process of laminated composite sheets for total deformation of  $\epsilon_z = 12\%$  and  $\epsilon_z = 18\%$ .

## MATHEMATICAL MODEL

Based on the literature analysis [27–29], simple one- and two-parameter models, such as the Maxwell model shown in Figure 4 or the Voigt model, do not correctly describe the actual conditions of the rolling process of composite products. The Maxwell model is a serial combination of Hooke’s and Newton’s models. Maxwell’s model allows for the analysis of relaxation but does not correctly reflect the creep phenomenon [6, 29]. Based on the work [26], it was found that for Maxwell’s model, the strains increase indefinitely for a constant value of stress, which does not occur in typical solids.

The classical linear theory of elasticity is based on Hooke’s law. It was assumed that the relationships between stress and strain are linear and independent of time [31, 32]. However, based on the works [6, 33], it was found that metals do

**Table 1.** Chemical composition of alloys (wt. [%])

Material	Al.	Mg	Cu	Zn	Ti	Si	Mn	Fe
AlMg	the rest	5.8	0.10	0.25	0.15	0.4	0.60	0.40
Al1050	the rest	0.047	0.05	0.008	0.05	0.06	0.005	0.32
M1E	-	-	the rest	0.003	0.002	0.002	-	0.005



**Figure 2.** View of the composite sample after joining by explosive welding



**Figure 3.** View of the duo rolling mill φ150 mm

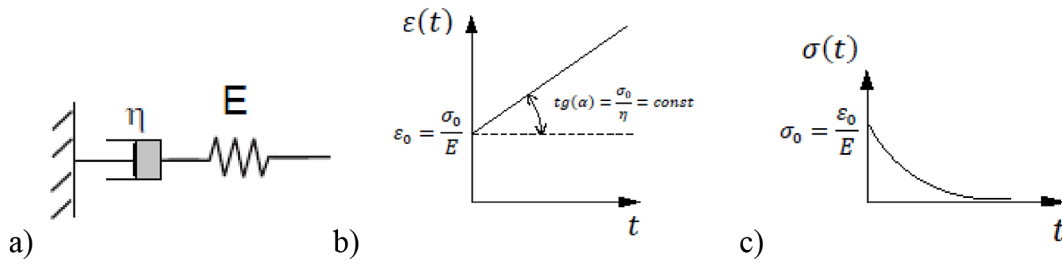


Figure 4. Maxwell's model (a) diagram, (b) creep curve, (c) relaxation curve [26–29]

not fully obey Hooke's law. An example here is the case of vibrations of metal bodies, which last infinitely long. Another case known from many experimental studies for many materials may be its loading for a long time. As a result of this action, it was observed that the deformations increase with the time of the material load [34, 35]. Therefore, the assumptions of the linear theory of elasticity should be supplemented with the time factor in the equations of state. Then the equation of state is described by a functional relationship in the form [27]:

$$f(\sigma, \varepsilon, t) = 0 \tag{1}$$

where:  $\sigma$  – stress,  $\varepsilon$  – strain,  $t$  – time.

The perfectly elastic body model and the viscous fluid model are used to describe viscoelastic bodies [36, 37]. Elastic effects, as previously mentioned, are subject to Hooke's law. However, the viscous effect obeys Newton's law [38, 39]. The combination of the linear theory of elasticity with viscous fluid mechanics was called the linear theory of viscoelasticity [40, 41]. In the linear theory of viscoelasticity, models composed of springs and dampers are used to describe the changes that occur during deformation [6, 27]. These models describe the behavior of an infinitesimal body element [29].

This work assumes small deformations and limits them to bodies subject to Boltzmann's superposition principle. In the further part of the work, the considerations will concern Boltzmann bodies, i.e. viscoelastic bodies with linear characteristics. The principle of superposition proposed by Boltzmann will constitute a heuristic law that is the basis for the mathematical description of the theory of viscoelastic bodies with linear characteristics. Based on the principle of superposition [6, 27], it was assumed that if stresses  $\sigma_1(t)$  cause material deformations  $\varepsilon_1(t)$  and if stresses  $\sigma_2(t)$  cause material deformations  $\varepsilon_2(t)$ , then the sum of these stresses  $\sigma_1(t) + \sigma_2(t)$  will cause the sum of deformations  $\varepsilon_1(t) + \varepsilon_2(t)$ .

The mechanical properties of a viscoelastic body are measured in two functions, i.e., the creep function (Figure 6) and the relaxation function (Figure 7). The creep function from the physical side is the elongation caused by applying a unit force at time  $t = 0$ . The applied force is the Heviside function, which is equal to zero for time  $t < 0$ , while for  $t \geq 0$  it is equal to unity. Regarding the relaxation function, it is the force causing elongation. This elongation is zero for  $t < 0$ , and when  $t \geq 0$ , it equals unity.

One of the simplest examples of relaxation and creep functions is stretching or compressing a rod made of viscoelastic material. Based on the work [6, 27], the concept of these functions was discussed on the example of stretching a rod made of viscoelastic material. Thus, the rod,

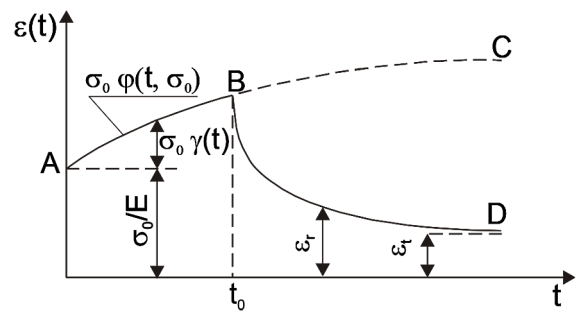


Figure 5. Creep function of a viscoelastic body [6, 29]

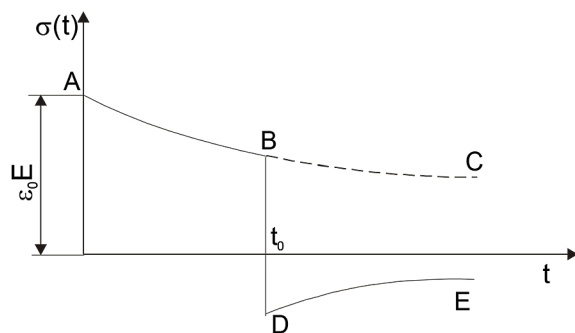
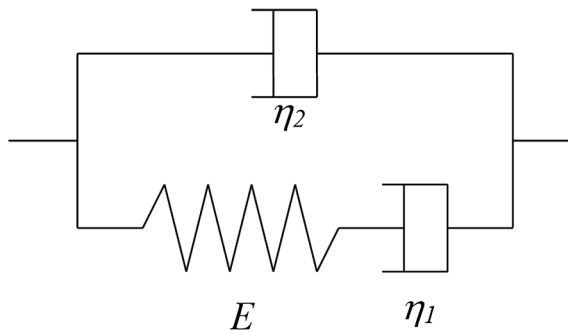


Figure 6. Relaxation function of a viscoelastic body [6, 29]



**Figure 7.** Schematic of the Jeffreys model [6, 28]:  
 $E$  – longitudinal modulus of elasticity,  
 $\eta_1, \eta_2$  – viscosity coefficients

which was at rest, was loaded at time  $t = 0$  with a force causing a stress  $\sigma_0$  in the rod, and the material's behavior at time  $t$  was examined. Therefore, the case of the function [6, 29] was considered:

$$\frac{\varepsilon(t)}{\sigma_0} = \varphi(t; \sigma_0) \quad (2)$$

Figure 5 shows that at the beginning, the deformation increases to the value marked at point A. This value is defined as:

$$\varepsilon(0^+) = \frac{\sigma_0}{E} \quad (3)$$

where:  $E$  – dynamic modulus of elasticity.

According to the AB and BC curves, the deformation increases with time in the next stage. Hence, the total deformation at time  $t$  is [6, 29]:

$$\varepsilon(t) = \varepsilon(0^+) + \varepsilon_p(t) = \frac{\sigma_0}{E} + \sigma_0 \gamma(t) \quad (4)$$

Therefore

$$\varphi(t; \sigma_0) = \frac{1}{E} + \gamma(t) = \varphi(0; \sigma_0) + \gamma(t) \quad (5)$$

Since the creep function does not depend on the place or shape of the body but only on time, it can be considered a function characterizing the rheological properties of a viscoelastic body. Moreover, it should be noted that if  $\gamma = 0$ , only elastic deformation occurs for any time  $t$ .

However, if at the moment  $t = t_0$  the material is unloaded, the deformation will gradually decrease until it reaches the value of permanent deformation  $\varepsilon_r$ . The BD curve shows the nature of the strain change, which is called the recovery curve of a viscoelastic material.

The relaxation function of a viscoelastic material is described by the relationship [6, 29]:

$$\frac{\sigma(t)}{\varepsilon_0} = \psi(t; \varepsilon_0) \quad (6)$$

Figure 7 shows the form of the relaxation function of a viscoelastic body.

In the tensile sample at  $t = 0$ , a finite strain  $\varepsilon_0$  is applied. The deformation at  $t = 0$  causes the stresses in the tensile sample to increase rapidly and reach the value [6, 29]:

$$\sigma(0^+) = \varepsilon_0 E \quad (7)$$

Then, we observe that the stress value decreases with the loading time according to the ABC curve, which we write as [6, 29]:

$$\sigma(t) = \sigma(0^+) + \varepsilon_0 V_r(t) \quad (8)$$

and

$$\psi(t, \varepsilon_0) = E + V_r(t) \quad (9)$$

Since the relaxation curve shown in Figure 6 is convex downwards, the derivative of the relaxation function is negative. However, if at the moment  $t=t_0$ , the load causing the deformation  $\varepsilon_0$  is removed, then the course of stress changes over time is illustrated by the ABDE curve.

Since one- and two-parameter models are insufficient to describe the deformation process of solids, three-parameter models are used for modern solutions [6, 29]. The application of Maxwell and Voight models do not describe the rolling process correctly. In current solutions, the most common models are three-, four- or more parameter ones. In this work, the combined three-parameter Jeffreys model [27, 28] was adopted for the considerations - to describe each of the components of the layered metal composite. This model allows for the analysis of independent deformation of the layers constituting the bimetal. In particular, the Jeffreys model consists of Maxwell and Newton models connected in parallel.

The equation of state for the Jeffreys model is described as [29]:

$$\left( \frac{1}{E} \frac{\partial}{\partial t} + \frac{1}{\eta_1} \right) \sigma_J(t) = \left( \left( 1 + \frac{\eta_2}{\eta_1} \right) \frac{\partial}{\partial t} + \frac{\eta_2}{E} \frac{\partial^2}{\partial t^2} \right) \varepsilon_J(t) \quad (10)$$

For the components of the layered composite, a parallel connection of three three-parameter Jeffreys models was assumed – Figure 7.

Determining the behavior of such a system is possible when we know the nine constants  $E_{AIMg}$ ,  $\eta_{1AIMg}$ ,  $\eta_{2AIMg}$ ,  $E_{Al1050}$ ,  $\eta_{1Al1050}$ ,  $\eta_{2Al1050}$ ,  $E_{MIE}$ ,  $\eta_{1MIE}$ ,  $\eta_{2MIE}$  describing the mechanical properties of the metals included in the layered composite. These constants denote the moduli of longitudinal elasticity and viscosity of individual composite layers, respectively.

The equation of state for the adopted model is formula 11 above.

$$\left. \begin{aligned} \left(\frac{1}{E_{AlMg}} \frac{\partial}{\partial t} + \frac{1}{\eta_{1AlMg}}\right) \sigma_{JAlMg}(t) &= \left[ \left(1 + \frac{\eta_{2AlMg}}{\eta_{1AlMg}}\right) \frac{\partial}{\partial t} + \frac{\eta_{2AlMg}}{E_{AlMg}} \frac{\partial}{\partial t^2} \right] \varepsilon_{JAlMg}(t) \\ \left(\frac{1}{E_{Al1050}} \frac{\partial}{\partial t} + \frac{1}{\eta_{1Al1050}}\right) \sigma_{JAl1050}(t) &= \left[ \left(1 + \frac{\eta_{2Al1050}}{\eta_{1Al1050}}\right) \frac{\partial}{\partial t} + \frac{\eta_{2Al1050}}{E_{Al1050}} \frac{\partial}{\partial t^2} \right] \varepsilon_{JAl1050}(t) \\ \left(\frac{1}{E_{M1E}} \frac{\partial}{\partial t} + \frac{1}{\eta_{1M1E}}\right) \sigma_{JM1E}(t) &= \left[ \left(1 + \frac{\eta_{2M1E}}{\eta_{1M1E}}\right) \frac{\partial}{\partial t} + \frac{\eta_{2M1E}}{E_{M1E}} \frac{\partial}{\partial t^2} \right] \varepsilon_{JM1E}(t) \end{aligned} \right\} \quad (11)$$

The Jeffreys model presented in Figure 8 applies to the arrangement of composite layers during the rolling process (Figure 9). On this basis, calculations were made of the deformations of individual layers in the rolling valley and the zone of delayed viscoelastic effects.

### RESULTS

As part of modeling the laminated composite sheets' rolling process, calculations were made for total deformation of  $\varepsilon = 12\%$  and  $\varepsilon = 18\%$ . The Mathcad computer program was used for numerical calculations. Figures 10 and 11 show the course of changes in the deformation of the components of the three-layer composite.

Based on the results presented in Figures 10 and 11, it can be observed that the values of deformations of composite components decrease after leaving the rolling gap. The values of deformations and their changes in the zone of delayed viscoelastic effects strictly depend on their properties. As a result of the existence of delayed viscoelastic effects, there is a differentiation of the values of deformations of composite layers in the zone of intensive deformations and the zone of delayed viscoelastic effects. Moreover, based on the presented test results, it can be concluded that the dependence of the deformation values of the layers constituting the composite on time is

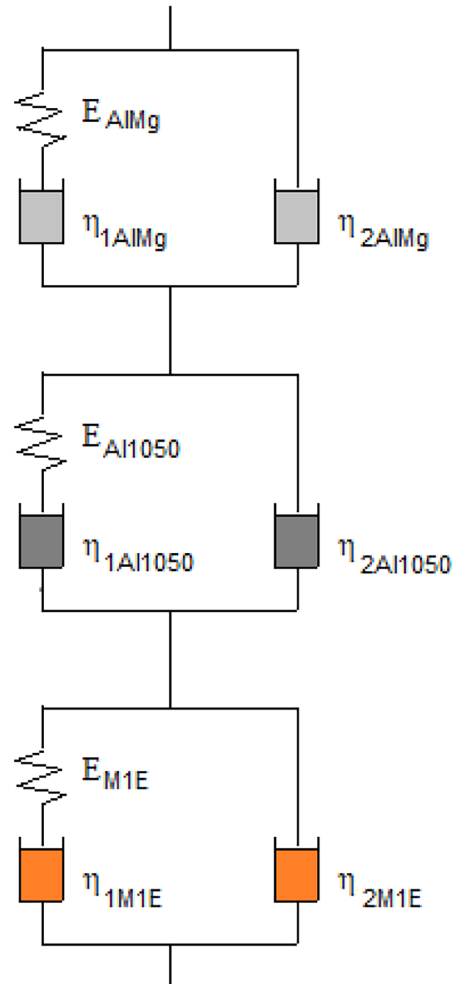


Figure 8. Jeffreys's model of the rolling process of a two-layer viscoelastic body

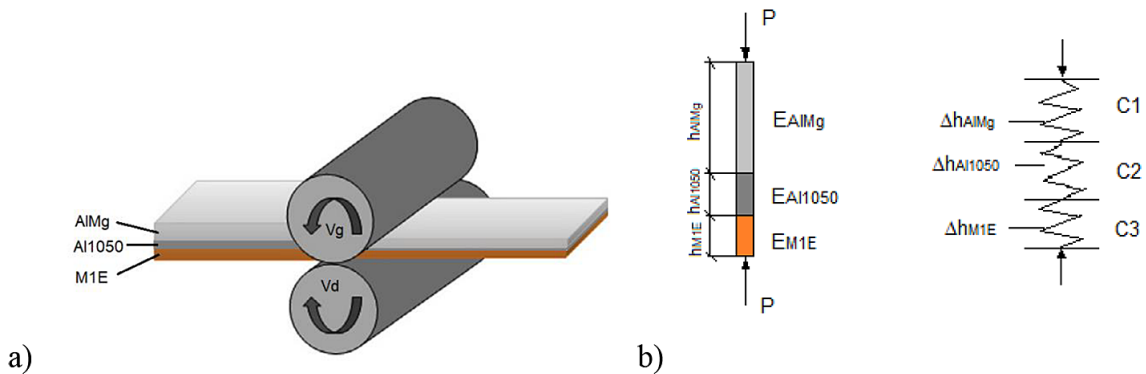


Figure 9. Scheme of shaping layered composites (a) rolling process, (b) fiber arrangement

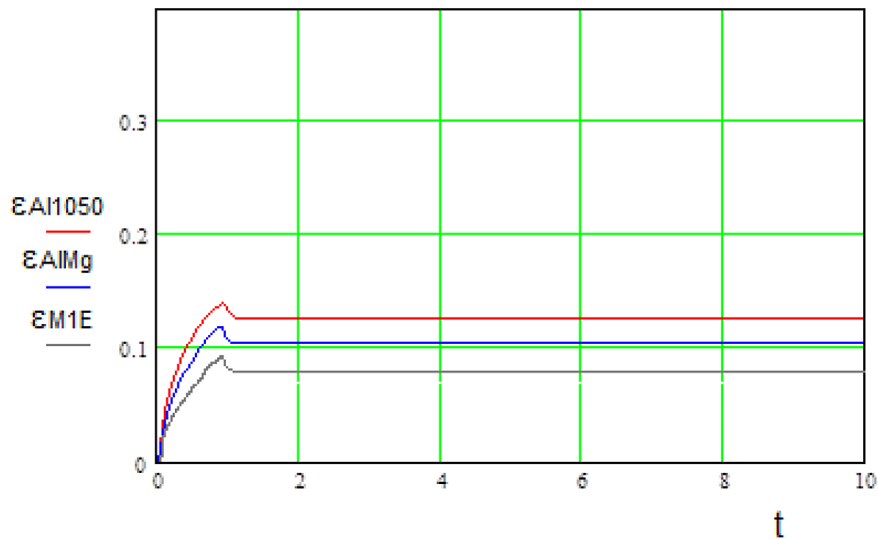


Figure 10. Distribution of viscoelastic strains in the rolling process of laminated composite sheets for  $\epsilon_z=12\%$

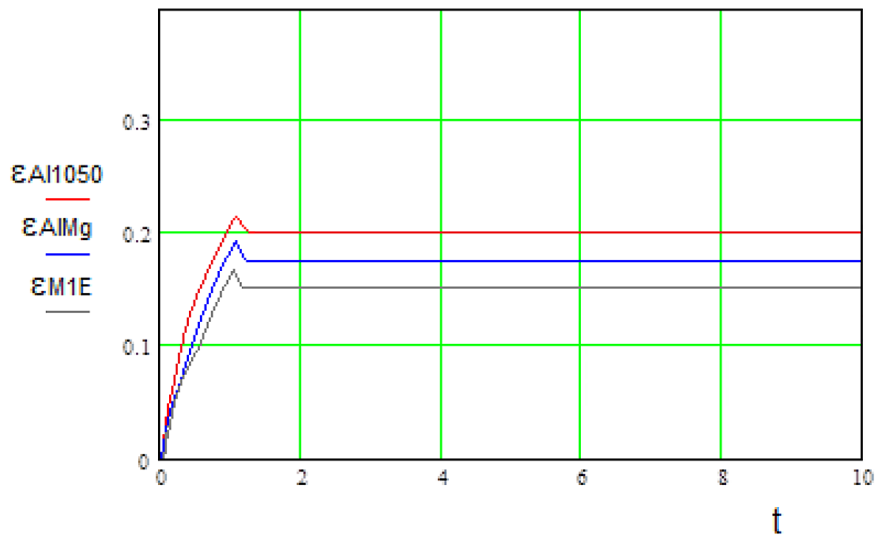
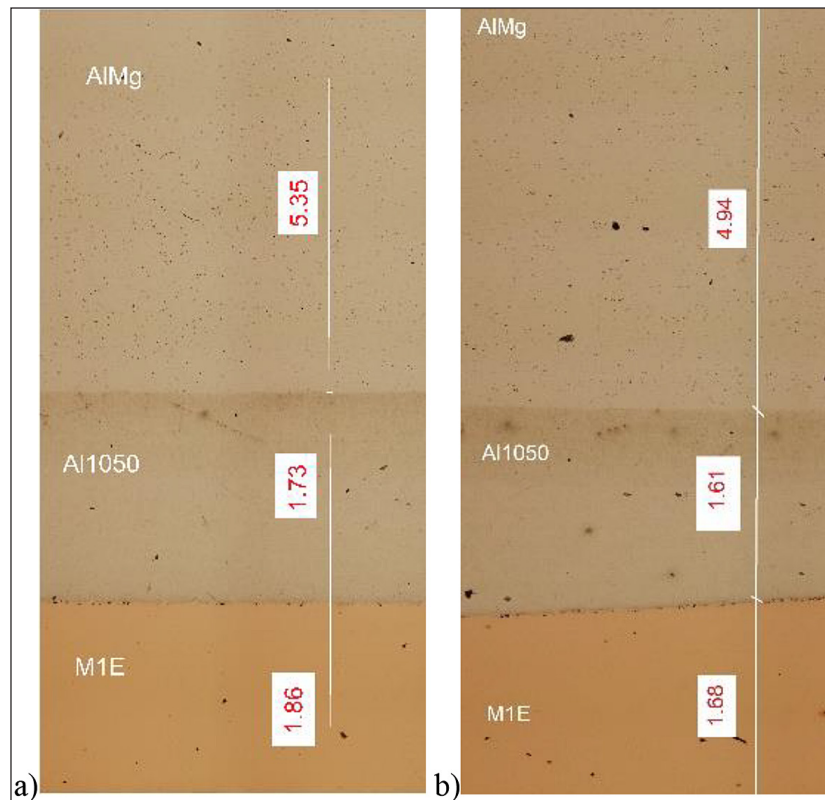


Figure 11. Distribution of viscoelastic strains in the rolling process of laminated composite sheets for  $\epsilon_z=18\%$

a linear function. This allows us to state that the conditions of Boltzmann’s principle are met, and the rolling of layered composites can be treated as multilayer linear viscoelastic bodies. The differences in the deformation values of the layers obtained on the basis of laboratory compression tests and calculated for the rolling process using the developed model show high compliance. A rolling process was carried out analogously in laboratory conditions to determine the correctness of the calculations. The results of layer thickness measurements are shown in Figure 12.

Figure 12 shows the results of thickness measurements of the layers constituting the AlMg+Al1050+M1E composite. The results presented in Figure 12 show that there is practically

no intermediate layer in the area where AlMg and Al1050 are joined. In contrast, in the case of the connection of Al1050 and M1E layers, there is an intermediate layer that was not deformed during the rolling process. Therefore, their occurrence was omitted in the overall calculations. Table 2 presents the results of computational and laboratory tests for rolling three-layer composite sheets with total relative deformation of  $\epsilon_z = 12\%$  and  $\epsilon_z = 18\%$ . Based on the presented computational test results and laboratory verification, it can be concluded that greater computational accuracy was achieved by considering delayed viscoelastic effects. The error in determining the value of permanent deformation of components of rolled layered composites did not exceed 1%.



**Figure 12.** Results of measuring the thickness of composite layers after the rolling process (a)  $\epsilon_z = 12\%$ , (b)  $\epsilon_z = 18\%$

**Table 2.** Summary of calculation and measurement results

Material	Initial dimensions			Calculation results					Laboratory results	
	$h_0$ mm	$b_0$ mm	$l_0$ mm	$h_1$ mm	$h_t$ mm	$\epsilon_z$ %	$\epsilon_1$ %	$\epsilon_2$ %	$h_t$ mm	$\epsilon_t$ %
AlMg	6	120	200	5.25	5.38	12	12.50	10.33	5.35	10.83
Al1050	2	120	200	1.73	1.75		13.50	12.50	1.73	13.00
M1E	2	120	200	1.80	1.86		10.00	7.00	1.85	7.50
AlMg	6	120	200	4.92	4.95	18	18.00	17.50	4.94	17.67
Al1050	2	120	200	1.62	1.63		19.00	18.50	1.62	19.00
M1E	2	120	200	1.66	1.68		17.00	16.00	1.68	16.00

**Note:**  $\epsilon_z$  – total relative deformation of the layered composite,  $\epsilon_1$  – relative deformation of the laminated composite layers in the rolling gap,  $\epsilon_t$  – (permanent) plastic relative deformations of the layers of the laminated composite.

## CONCLUSIONS

This paper presents a new solution for the rolling of composite laminated sheets, based on the assumptions of a viscoelastic medium. The proposed application of the viscoelastic theory to the analysis of the rolling process of laminated composites has not been previously observed in a literature review. A mathematical model developed as part of the work was used for theoretical analysis based on the Jeffreys rheological model. The course of changes in the deformation of the composite layers in the zone of intense deformation and delayed viscoelastic effects was analyzed.

Experimental verification of the calculation results based on the mathematical model presented in this work demonstrated the possibility of correctly predicting the deformations of the sandwich composite layers. The results presented in this paper prove that the use of the theory of viscoelasticity leads to an increase in the accuracy of calculations compared to the results obtained using the finite element method. As a result of the expansion of the materials constituting the layered composite, the deformation value of each layer changes. The applied solution of the viscoelastic theory enables the observation of the course of deformation changes in the rolling gap

and after leaving it. The solution proposed in the work is important both due to the accuracy of the calculations and the cognitive character of the behavior of materials during the rolling process.

Based on the presented calculation results and the experimental verification, it can be concluded that the intended goal of the work was achieved. By comparing the results of calculations of deformations in the zone of intense deformations  $\epsilon_1$  and calculations of permanent deformations in the zone of delayed viscoelastic effects  $\epsilon_t$ , it can be concluded that after taking into account the occurrence of delayed viscoelastic effects, the accuracy of the calculations increases.

## REFERENCES

- Podulka, P., Macek, W., Szala, M., Kubit, A., Das, K.C., Królczyk, G. Evaluation of high-frequency roughness measurement errors for composite and ceramic surfaces after machining. *Journal of Manufacturing Processes* 2024, 121, 150–171. <https://doi.org/10.1016/j.jmapro.2024.05.032>
- Sawa, M., Szala, M., Jakliński, P., Pietrykowski, K. Airframe design and CFD analysis of light unmanned reconnaissance aircraft. *J. Phys.: Conf. Ser.* 2022, 2412, 012013. <https://doi.org/10.1088/1742-6596/2412/1/012013>
- Szala, M.; Walczak, M. Metallic and Ceramic Materials Integrity—Surface Engineering for Wear, Corrosion and Erosion Prevention. *Materials* 2024, 17, 1541. <https://doi.org/10.3390/ma17071541>
- Próchniak, M. The analysis of institutional environment in the area of product market competition in the new EU member states: What do the data say about the models of capitalism emerging in the CEE countries? *International Journal of Management and Economics* 2018, 54, 304–327. <https://doi.org/10.2478/ijme-2018-0029>
- Próchniak, M. An attempt to assess the quantitative impact of institutions on economic growth and economic development. *International Journal of Management and Economics* 2014, 38, 7–30. <https://doi.org/10.2478/ijme-2014-0012>
- Rydz, D. Analiza procesu walcowania blach bimetalowych z zastosowaniem rozwiązań dla ciał lepkosprężystych „Analysis of the rolling process of bimetal sheets using solutions for viscoelastic bodies”, Monograph no. 152, Częstochowa University of Technology, 2009.
- Skowrońska, B., Chmielewski, T., Zasada, D. Assessment of Selected Structural Properties of High-Speed Friction Welded Joints Made of Unalloyed Structural Steel. *Materials* 2022, 16, 93, <https://doi.org/10.3390/ma16010093>
- Skowrońska, B., Chmielewski, T., Kulczyk, M., Skiba, J., Przybysz, S. Microstructural Investigation of a Friction-Welded 316L Stainless Steel with Ultrafine-Grained Structure Obtained by Hydrostatic Extrusion. *Materials* 2021, 14, 1537, <https://doi.org/10.3390/ma14061537>
- Skowrońska, B., Bober, M., Kołodziejczak, P., Baranowski, M., Kozłowski, M., Chmielewski, T. Solid-state rotary friction-welded tungsten and mild steel joints. *Applied Sciences* 2022, 12, 9034, <https://doi.org/10.3390/app12189034>
- Szczucka-Lasota, B., Szymczak, T., Węgrzyn, T., Tarasiuk, W. Superalloy—steel joint in microstructural and mechanical characterisation for manufacturing rotor components. *Materials* 2023, 16, 2862. <https://doi.org/10.3390/ma16072862>
- Tomasz Węgrzyn, T.W., Szczucka-Lasota, B., Tarasiuk, W., Cybulko, P., Jurek, A., Döring, A., Kosarac, A. Mag welding of duplex steel for the construction of antenna mounts. *Adv.Tech&Mat.* 2022, 47, 21–25. <https://doi.org/10.24867/ATM-2022-2-004>
- Oniszczyk-Świercz, D., Kopytowski, A., Nowicki, R., Świercz, R. Finishing additively manufactured Ti6Al4V alloy with low-energy electrical discharges. *Materials* 2023, 16, 5861. <https://doi.org/10.3390/ma16175861>
- Jonda, E.S., Fydrych, D., Łatka, L., Myalska-Głowacka, H. The use of cluster analysis to assess the wear resistance of cermet coatings sprayed by high velocity oxy-fuel on magnesium alloy substrate. *Adv. Sci. Technol. Res. J.* 2024, 18, 216–227. <https://doi.org/10.12913/22998624/188877>
- Kumar, A., Sirohi, S., Singh, M., Fydrych, D., Pandey, C. Microstructure and mechanical properties of a dissimilar metal welded joint of Inconel 617 and P92 steel with Inconel 82 buttering layer for AUSC boiler application. *International Journal of Pressure Vessels and Piping* 2024, 209, 105196. <https://doi.org/10.1016/j.ijpvp.2024.105196>
- Lu, T.A.V. Metrikine, M.J.M.M. Steenberg. The equivalent dynamic stiffness of a visco-elastic half-space in interaction with a periodically supported beam under a moving load. *European Journal of Mechanics - A/Solids.* 2020, 84, 104065,
- Rakshit, A.K., Sengupta P.R. Magneto-thermo-visco-elastic waves in an initially stressed conducting layer. *Sādhanā* 1998, 23, 233–246.
- Šulda, J., Adámek, V., Kroft R. Transient response of non-prismatic heterogeneous viscoelastic rods and identification of their material properties. *European Journal of Mechanics - A/Solids* 2024, 105,
- Terapabkajornded, Y., Orankitjaroen, S., Licht, C. Asymptotic model of linearly visco-elastic Kelvin–Voigt type plates via Trotter theory. *Advances in Difference Equations* 2019.

19. Medina-Lombardero, S., Bain, C., Charlton, L., Pelligo, A., Roccliffe, H., Cash, J., Reuben, R., Crichton, M.L. The biomechanics of wounds at physiologically relevant levels: Understanding skin's stress-shielding effect for the quantitative assessment of healing. *Materials Today Bio* 2024, 25, 100963.
20. Ewoldt, R.H., Hosoi, A.E., McKinley, G.H. New measures for characterizing nonlinear viscoelasticity in large amplitude oscillatory shear, *Journal of Rheology* 2008, 52(6), 1427–1458.
21. Zhang K., Zhu M., Thomas E., Hopyan S., Sun Y. Existing and potential applications of elastography for measuring the viscoelasticity of biological tissues in vivo. *Front. Physiol.* Jun. 2021, 9 <https://doi.org/10.3389/fphy.2021.670571>
22. Paul S. Biodynamic excisional skin tension lines for surgical excisions: untangling the science. *Ann. R. Coll. Surg. Engl.* Apr. 2018, 100(4), 330–337. <https://doi.org/10.1308/rcsann.2018.0038>
23. Szarek A, Stradomski G, Łukomska-Szarek J, Rydz D, Wolański W, Jozsko K. Wear Morphology on the Surfaces of CoCrMo Unicompartamental Knee Joint Endoprostheses as Elements of Metal–Metal Friction Nodes. *Materials*. 2020, 13(12), 2689. <https://doi.org/10.3390/ma13122689>
24. Ceglie, M., Menga, N., Carbone, G. Modelling the non-steady peeling of viscoelastic tapes. *International Journal of Mechanical Sciences* 2024, 267.
25. Zhang, Z., Chen, Y., Han, K., Wei, G., Pan, Y., Sun, M. Mathematical modelling for interaction between soft ground and small curvature shield tunneling considering viscoelastic characteristics influences. *Applied Mathematical Modelling* 2024, 127, 607–639.
26. Rydz, D., Stradomski, G., Dyja, H. Influence of relative rolling reduction and thickness layers bimetallic plate at the non-uniformity of the strain after rolling process. *IOP Conference Series: Materials Science and Engineering* 2017, 179, 012062.
27. Nowacki W. Postępy w teorii sprężystości, Warszawa, PWN 1986.
28. Jeffreys, H. *The Earth*, Cambridge University Press, 1960.
29. Nowacki, W. *Theory of asymmetrical elasticity*, Warszawa, PWN/Oxford, Pergamon Press 1986.
30. Zhang, J, Kong, X, Cheng, L, Qi, H, Yu, M. Intelligent fault diagnosis of rolling bearings based on continuous wavelet transform-multiscale feature fusion and improved channel attention mechanism. *Eksploatacja i Niezawodność – Maintenance and Reliability*. 2023, 25(1), 16. <https://doi.org/10.17531/ein.2023.1.16>
31. Szczucka-Lasota, B., Węgrzyn, T., Jurek, A. Formation of Oxides and Sulfides during the Welding Process of S700MC Steel by Using New Electrodes Wires. *Materials* 2024, 17, 2974. <https://doi.org/10.3390/ma17122974>
32. Węgrzyn, T., Szczucka-Lasota, B., Szymczak, T. A micro-cooled high-strength weld for heavy transport means. *TP 2024b*, 19, 83–95. <https://doi.org/10.20858/tp.2024.19.1.07>
33. Skalmierski, B., Rydz, D. Zastosowanie rozwiązań lepkosprężystych do opisanego procesu walcowania blach. Seria: Metalurgia nr 39, V Międzyn. sesja naukowa: Nowe Technologie i Osiągnięcia w Metalurgii i Inżynierii Materiałowej, Częstochowa 2004.
34. Shew, W., Pinton, J-F. Viscoelastic effects on the dynamics of a rising bubble, *Journal of Statistical Mechanics: Theory and experiment*, 1–15, January 2006.
35. Rydz, D., Skalmierski, B., Stefanik, A., Kawalek, A. Theoretical analysis of the process of rolling flat products with the use of visco-elastic solutions, *Maszynostrojenie I Technosfera XXI Wieka, Sbornik Trudow XI Międzynarodowej Nauczno-Technicznej Konferencji*, 13–18.09.2004. Sewastopol.
36. Rathore, S., Kumar, A., Sirohi, S., Singh, V., Gupta, A., Fydrych, D., Pandey, C. Role of buttering layer composition on microstructural heterogeneity and mechanical properties of Alloy 617 and P92 steel dissimilar welded joints for future Indian AISC program. *Int J Adv Manuf Technol* 2024, 133, 671–700. <https://doi.org/10.1007/s00170-024-13747-w>
37. Oniszczyk-Świercz, D., Świercz, R., Kopytowski, A., Nowicki, R., Experimental investigation and optimization of rough EDM of high-thermal-conductivity tool steel with a thin-walled electrode. *Materials* 2022, 16, 302. <https://doi.org/10.3390/ma16010302>
38. Węgrzyn, T., Gołombek, K., Szczucka-Lasota, B., Szymczak, T., Łazarz, B., Łukaszewicz, K. Docol 1300M micro-jet-cooled weld in microstructural and mechanical approaches concerning applications at cyclic loading. *Materials* 2024a, 17, 2934. <https://doi.org/10.3390/ma17122934>
39. Kopytowski, A., Świercz, R., Oniszczyk-Świercz, D., Zawora, J., Kuczak, J., Żrodowski, Ł. Effects of a new type of grinding wheel with multi-granular abrasive grains on surface topography properties after grinding of inconel 625. *Materials* 2023, 16, 716. <https://doi.org/10.3390/ma16020716>
40. Skowrońska, B., Chmielewski, T., Baranowski, M., Kulczyk, M., Skiba, J., Friction weldability of ultra-fine-grained titanium grade 2. *Journal of Advanced Joining Processes* 2024a, 10, 100246. <https://doi.org/10.1016/j.jajp.2024.100246>
41. Skowrońska, B., Szulc, B., Morek, R., Baranowski, M., Chmielewski, T.M., Selected properties of X120Mn12 steel welded joints by means of the plasma-MAG hybrid method. *Proceedings of the Institution of Mechanical Engineers, Part L: Journal of Materials: Design and Applications* 2024b, 14644207241256113. <https://doi.org/10.1177/14644207241256113>